

# Overview of the FTU results

**G. Pucella**

on behalf of FTU Team and Collaborators

presented by: ***G. Calabrò***

Unità Tecnica Fusione, ENEA C. R. Frascati, Frascati, Italy

IFP-CNR, Istituto di Fisica del Plasma, Milano, Italy

Consorzio CREATE, Università di Napoli Federico II, Napoli, Italy

Dip. Ing. Civile e Ing. Informatica, Università di Roma Tor Vergata, Roma, Italy

Dip. Energetica, Politecnico di Milano, Milano, Italy

UTAPRAD, ENEA C. R. Frascati, Frascati, Italy

Ecole Polytechnique Fédérale de Lausanne, CRPP, Lausanne, Switzerland

National Centre for Nuclear Research (NCBJ), Swierk, Poland

Universidad Carlos III de Madrid, Madrid, Spain

JSC Red Star, Moscow, Russian Federation

F4E: Fusion for Energy, Barcelona, Spain

## ☐ Introduction

## ☐ Experimental results

## ☐ Contributions

### ☐ Runaway electrons generation and control

- Threshold electric field for runaway electron generation (EX/P2-50)
- Runaway electrons control (EX/P2-48)

### ☐ ECW experiments

- Real time control of MHD instabilities (EX/P2-47)
- Amplification of (N)TM by central EC power (EX/P2-54)
- EC assisted plasma start-up (EX/P2-51)

### ☐ Lithium Limiter experiments

- Thermal load on the new lithium limiter (EX/P2-46)
- Elongated plasmas

### ☐ Plasma response to neon injection

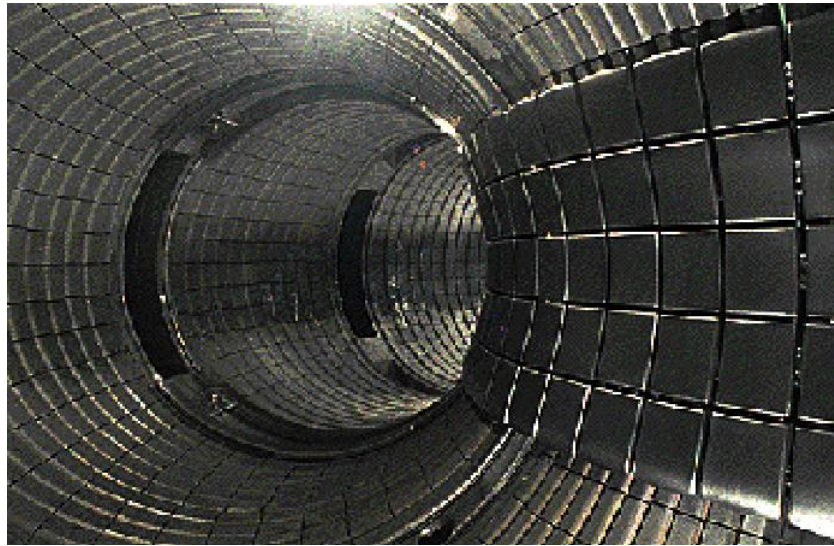
- Peaked density profiles (EX/P2-52)
- Tearing mode instabilities (EX/P2-53)

### ☐ MHD signals as disruption precursors

### ☐ Scrape-Off Layer studies

### ☐ Diagnostics

- Cherenkov probe (EX/P2-49)
- Gamma camera
- Laser Induced Breakdown Spectroscopy



## Compact high magnetic field machine

$R_0$	0.935	m	<i>Major radius</i>
$a$	0.30	m	<i>Minor radius</i>
$B_T$	$2 \div 8$	T	<i>Toroidal field</i>
$I_p$	$0.2 \div 1.6$	MA	<i>Plasma current</i>
$n_e$	$0.2 \div 4.0$	$10^{20} \text{ m}^{-3}$	<i>Plasma density</i>
$\Delta t$	1.5	s	<i>Pulse duration</i>
<b>EC</b>	140 GHz / 1.5 MW		<i>Electron Cyclotron</i>
<b>LH</b>	8 GHz / 2.0 MW		<i>Lower Hybrid</i>

- Stainless steel vacuum chamber
- High field side Mo belt limiter
- Outer Mo poloidal limiter
- Li poloidal limiter

☐ Introduction

☒ Experimental results

☐ Contributions

☒ **Runaway electrons generation and control**

- Threshold electric field for runaway electron generation (EX/P2-50)
- Runaway electrons control (EX/P2-48)

☐ **ECW experiments**

- Real time control of MHD instabilities (EX/P2-47)
- Amplification of (N)TM by central EC power (EX/P2-54)
- EC assisted plasma start-up (EX/P2-51)

☐ **Lithium Limiter experiments**

- Thermal load on the new lithium limiter (EX/P2-46)
- Elongated plasmas

☐ **Plasma response to neon injection**

- Peaked density profiles (EX/P2-52)
- Tearing mode instabilities (EX/P2-53)

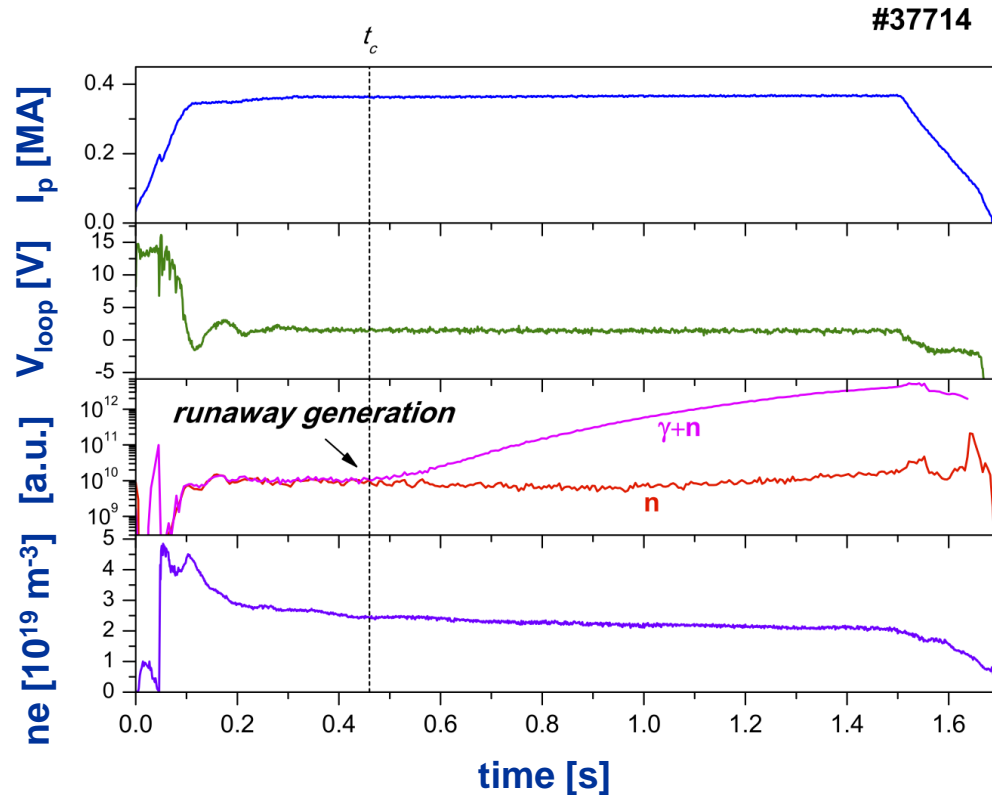
☐ **MHD signals as disruption precursors**

☐ **Scrape-Off Layer studies**

☐ **Diagnostics**

- Cherenkov probe (EX/P2-49)
- Gamma camera
- Laser Induced Breakdown Spectroscopy

# Runaway electrons generation



□ Conditions for RE generation in ohmic pulses investigated for a wide range of toroidal magnetic fields and plasma currents.

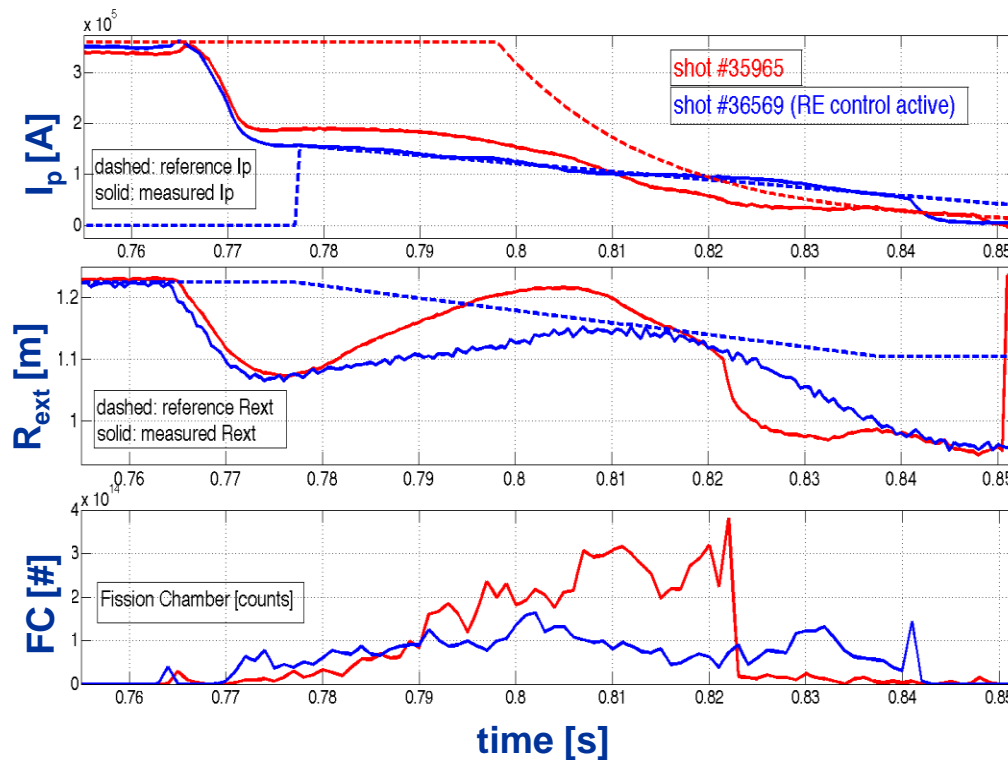
□ Critical electric field for RE generation 2÷5 times larger than the one from collisional theory.

□ Results agree with the new threshold calculated including synchrotron radiation losses.

□ **Determination of the threshold density value to be achieved by means of massive gas injection for RE suppression in ITER.**

**Esposito B. IAEA EX/P2-50 (2014)**

# Runaway electrons control

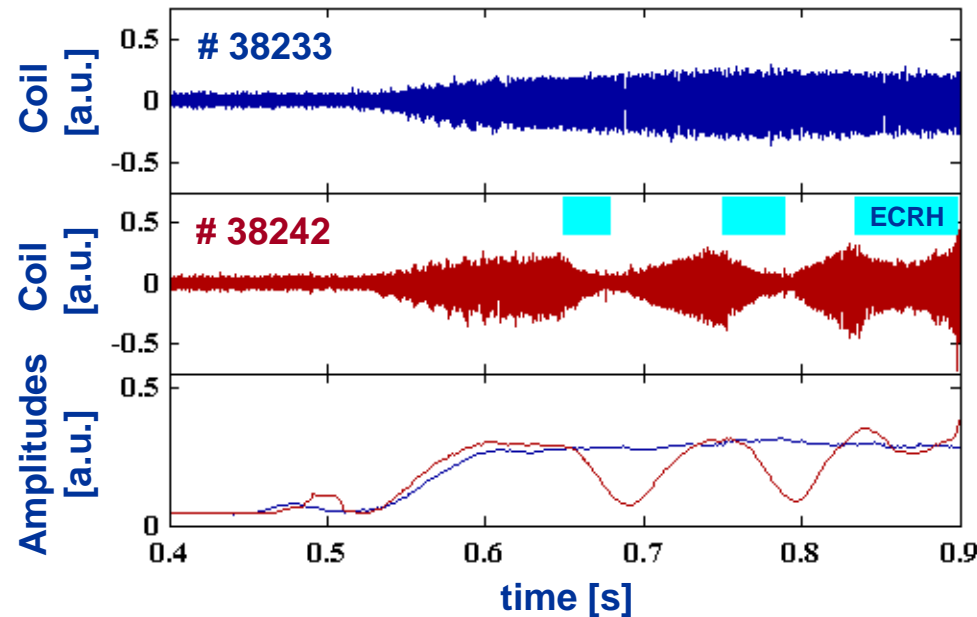


- ☐ New RE control algorithm tested for real-time control of disruption-generated RE beam.
- ☐ Minimize interaction with plasma facing components while RE current is ramped-down by induction.
- ☐ Fission chambers signals show reduced plasma facing components interaction with the new controller.

☐ **Reduction of the dangerous effects of RE during disruptions in ITER operation.**

**Carnevale D. IAEA EX/P2-48 (2014)**

- ☐ Introduction
- ☒ Experimental results
  - ☐ Runaway electrons generation and control
    - Threshold electric field for runaway electron generation (EX/P2-50)
    - Runaway electrons control (EX/P2-48)
  - ☒ ECW experiments
    - Real time control of MHD instabilities (EX/P2-47)
    - Amplification of (N)TM by central EC power (EX/P2-54)
    - EC assisted plasma start-up (EX/P2-51)
  - ☐ Lithium Limiter experiments
    - Thermal load on the new lithium limiter (EX/P2-46)
    - Elongated plasmas
  - ☐ Plasma response to neon injection
    - Peaked density profiles (EX/P2-52)
    - Tearing mode instabilities (EX/P2-53)
  - ☐ MHD signals as disruption precursors
  - ☐ Scrape-Off Layer studies
  - ☐ Diagnostics
    - Cherenkov probe (EX/P2-49)
    - Gamma camera
    - Laser Induced Breakdown Spectroscopy
- ☐ Contributions



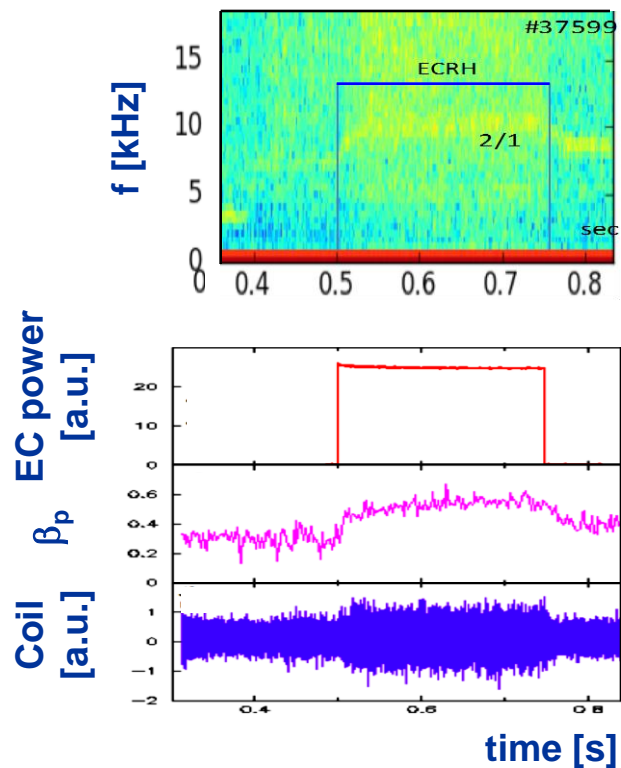
- ☐ Real time control of MHD instabilities using the new EC launcher with fast steering capability (1 deg / 10 ms).
- ☐ Low-order tearing modes induced by neon injection or by near-limit density.
- ☐ The data show a marked sensitivity of the resulting instability amplitude to the ECW deposition location.

☐ The experimental condition (control tools essential and based on a minimal set of diagnostics) mimics the situation of a fusion reactor.

**Sozzi C. IAEA EX/P2-47 (2014)**



# Amplification of (N)TM by central EC power



□ Amplification mechanisms by EC due to:

- Modification of the local plasma current density and of the mode stability parameter  $\Delta'_0$ .
- Increased bootstrap effect proportional to  $\beta_p$ .

2/1 NTM classification due to the instability amplification by increased bootstrap effect

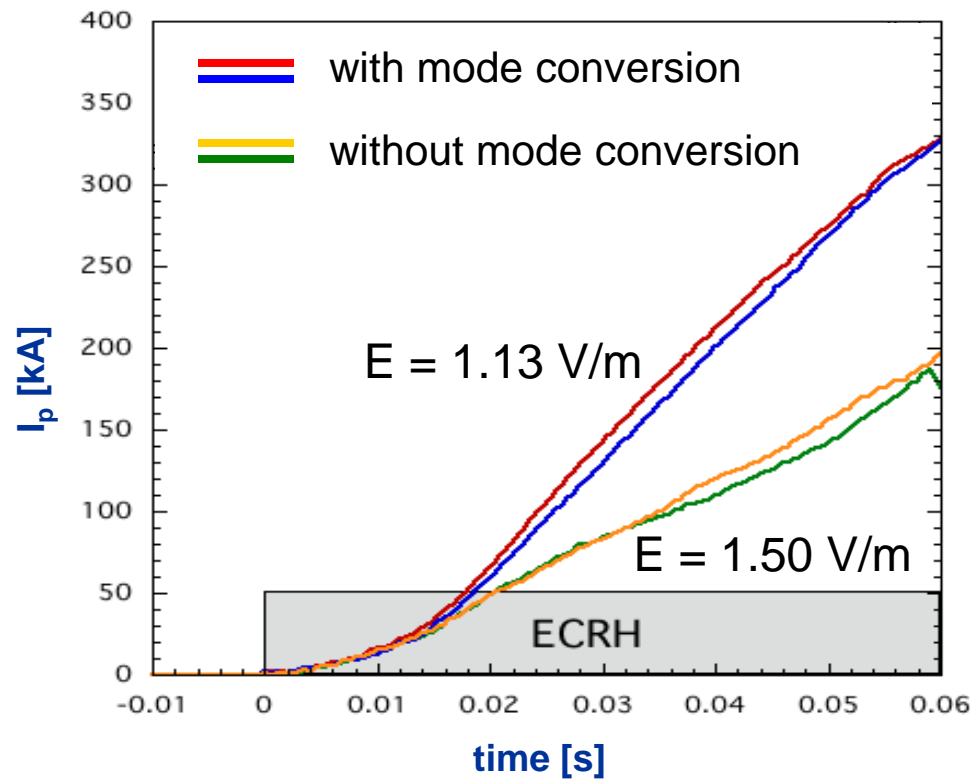
□ Frequency increase due to torque action originated from the applied co-ECCD.

No effect due to modification of rotation (ion polarization effect) because of the amplified size of existing perturbation.

□ **Important issue for the fusion plasma operations to avoid the degradation of the plasma confinement due to resistive instabilities.**

**Nowak S. IAEA EX/P2-54 (2014)**

# EC assisted plasma start-up



- ☐ Variations of launching angle: OX polarization conversion at reflection from inner wall  $\rightarrow$  better power absorption  $\rightarrow$  higher  $T_e \rightarrow$  lower resistivity.
- ☐ Variations of field null position via external vertical magnetic field.

☐ Experiments focused on ITER start-up issues: start-up at low toroidal electric field (0.5 V/m), even in presence of a large stray magnetic field (10 mT).

**Granucci G. IAEA EX/P2-51 (2014)**

☐ Introduction

☒ Experimental results

☐ Contributions

☐ Runaway electrons generation and control

- Threshold electric field for runaway electron generation (EX/P2-50)
- Runaway electrons control (EX/P2-48)

☐ ECW experiments

- Real time control of MHD instabilities (EX/P2-47)
- Amplification of (N)TM by central EC power (EX/P2-54)
- EC assisted plasma start-up (EX/P2-51)

☒ Lithium Limiter experiments

- Thermal load on the new lithium limiter (EX/P2-46)
- Elongated plasmas

☐ Plasma response to neon injection

- Peaked density profiles (EX/P2-52)
- Tearing mode instabilities (EX/P2-53)

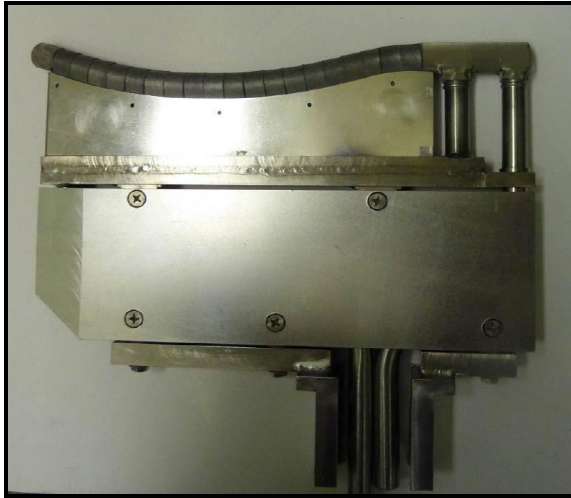
☐ MHD signals as disruption precursors

☐ Scrape-Off Layer studies

☐ Diagnostics

- Cherenkov probe (EX/P2-49)
- Gamma camera
- Laser Induced Breakdown Spectroscopy

# Thermal load on the new lithium limiter

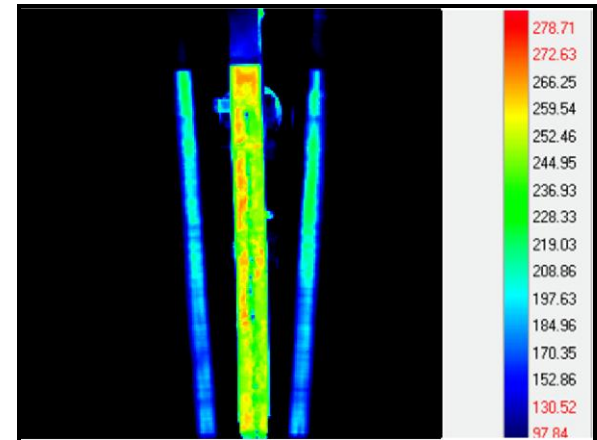


❑ New actively Cooled Lithium Limiter (CLL) with 200°C pressurized (30 bar) water circulation. 10 MW/m<sup>2</sup> target heat load.

❑ CLL inserted close to the LCMS (2 MW/m<sup>2</sup>), without any damage to the limiter surface.

❑ Heat load on the CLL from fast IR camera (■ 230°C).

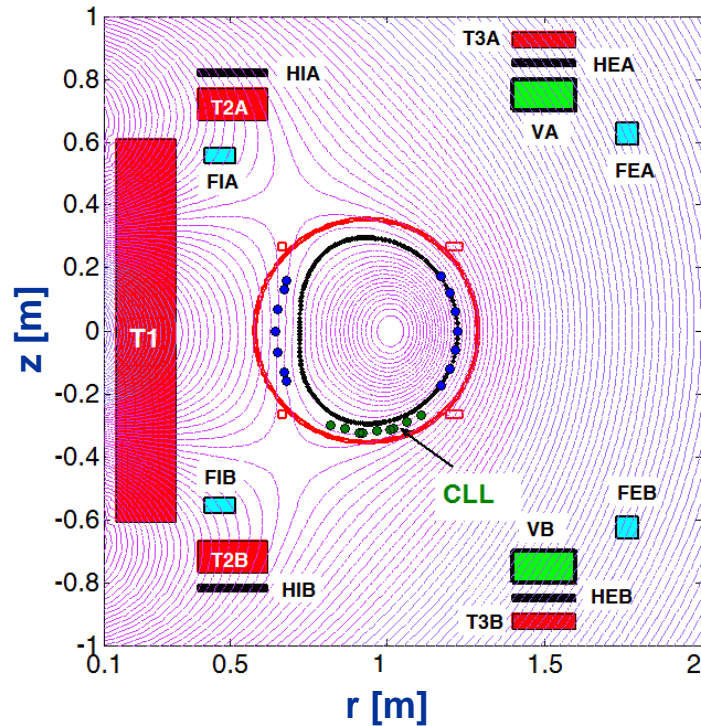
❑ 5 s dedicated pulses in preparation.



❑ **Liquid metals could be a viable solution for the problem of the power load on the divertor for steady state operation on the future reactors.**

**Mazzitelli G. IAEA EX/P2-46 (2014)**

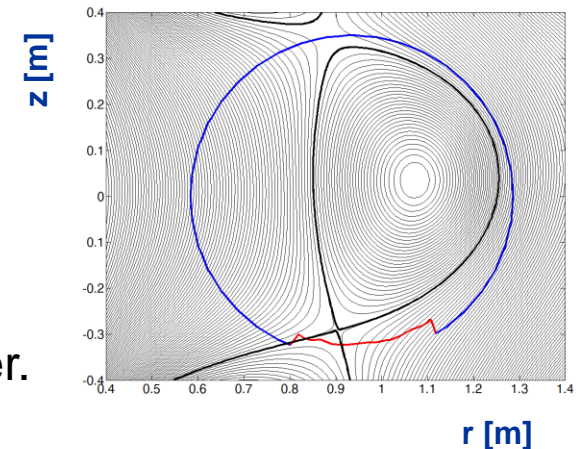
# Elongated plasmas



□ Elongated plasmas (5.5 T, 200 kA,  $k \sim 1.2$ ) with ECW additional heating (500 kW).

□ Vary local magnetic shear (flux surfaces opening) at the CLL.

□ Study on-going:  
X-point configuration with a magnetic single null inside the chamber.



□ Aim at investigating H-mode access, thus having the possibility to study the impact of ELMs on the CLL used as first limiter.

Calabrò G., EPS P4.005 (2014) – Ramogida G., SOFT P2.014 (2014)

☐ Introduction

☒ Experimental results

☐ Contributions

☐ **Runaway electrons generation and control**

- Threshold electric field for runaway electron generation (EX/P2-50)
- Runaway electrons control (EX/P2-48)

☐ **ECW experiments**

- Real time control of MHD instabilities (EX/P2-47)
- Amplification of (N)TM by central EC power (EX/P2-54)
- EC assisted plasma start-up (EX/P2-51)

☐ **Lithium Limiter experiments**

- Thermal load on the new lithium limiter (EX/P2-46)
- Elongated plasmas

☒ **Plasma response to neon injection**

- Peaked density profiles (EX/P2-52)
- Tearing mode instabilities (EX/P2-53)

☒ **MHD signals as disruption precursors**

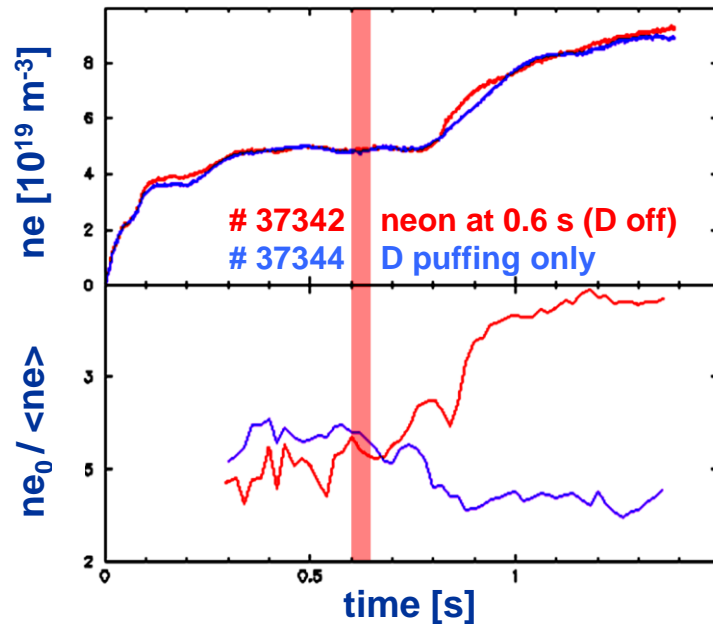
☒ **Scrape-Off Layer studies**

☐ **Diagnostics**

- Cherenkov probe (EX/P2-49)
- Gamma camera
- Laser Induced Breakdown Spectroscopy

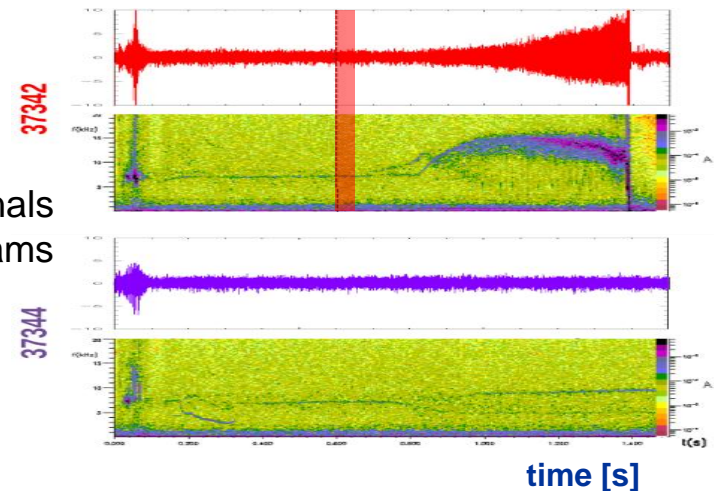


# Plasma response to neon injection



- ☐ Density peaking increases in response to neon puffing.
- ☐ More inward pinch than in the reference case at the same density without neon puffing.

Mirnov coil signals  
and Spectrograms

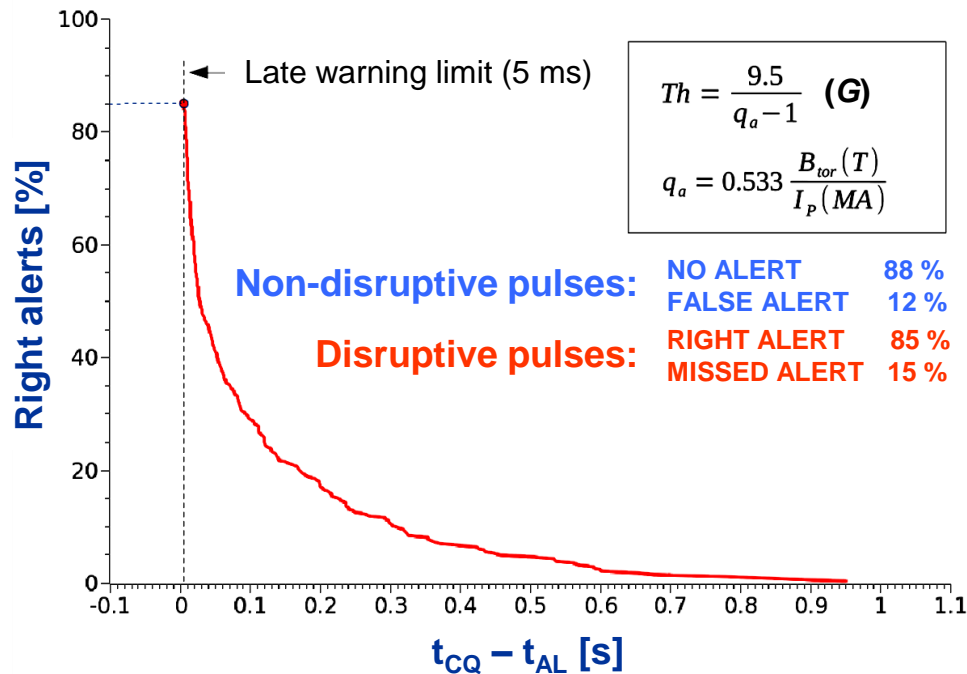


- ☐ Onset or amplification of low-order tearing modes.

☐ It is important to determine the conditions of an increase of particle confinement while minimizing the amount of impurities needed.

**Mazzotta C.** IAEA EX/P2-52 (2014)

**Botrugno A.** IAEA EX/P2-53 (2014)

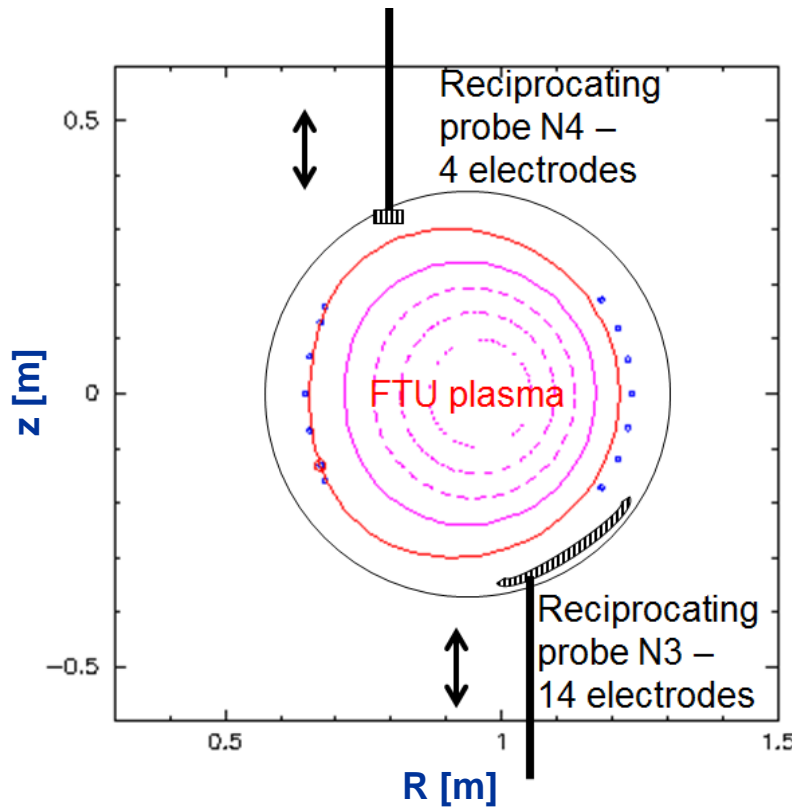


- ☐ Full real-time algorithm for disruption prediction, based on MHD activity signals from Mirnov coils.
- ☐ Threshold parameterization in terms of plasma parameters ( $B_T$ ,  $I_p$ ) optimized for maximum of timely right alerts and minimum of false alerts.
- ☐ Threshold optimization on 2000 pulses covering a wide range of physical parameters.

☐ The definition of suitable disruption precursors is of crucial importance in order to trigger actions for avoiding or at least mitigating disruptions.

Cianfarani C., EPS P5.165 (2013)





- Data collected by two arrays of reciprocating Langmuir probes.
- Scaling of the heat flux e-folding length  $\lambda$  in the scrape-off layer with:

- toroidal magnetic field ( $B_T$ )
- plasma current ( $I_p$ )
- line-averaged density ( $n_e$ )
- power to SOL ( $P_{SOL}$ )

Strong dependency of  $\lambda$  on  $I_p$  ( $\sim I_p^{0.6}$ )  
and  $P_{SOL}$  ( $\sim P_{SOL}^{-0.8}$ )

□ **This experiment contributed to the multi-tokamak scaling of SOL heat flux width of ITER limiter start-up plasma.**

Viola B., EPS P1.119 (2013)

☐ Introduction

☒ Experimental results

☐ Contributions

☐ **Runaway electrons generation and control**

- Threshold electric field for runaway electron generation (EX/P2-50)
- Runaway electrons control (EX/P2-48)

☐ **ECW experiments**

- Real time control of MHD instabilities (EX/P2-47)
- Amplification of (N)TM by central EC power (EX/P2-54)
- EC assisted plasma start-up (EX/P2-51)

☐ **Lithium Limiter experiments**

- Thermal load on the new lithium limiter (EX/P2-46)
- Elongated plasmas

☐ **Plasma response to neon injection**

- Peaked density profiles (EX/P2-52)
- Tearing mode instabilities (EX/P2-53)

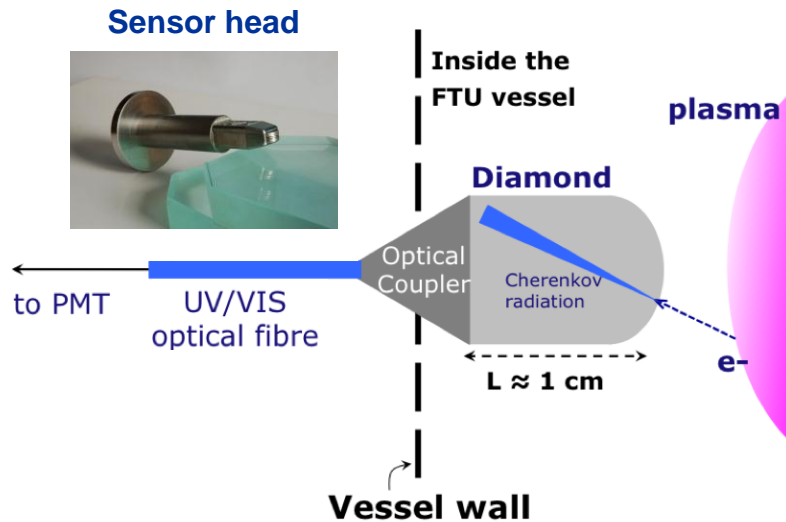
☐ **MHD signals as disruption precursors**

☐ **Scrape-Off Layer studies**

☒ **Diagnostics**

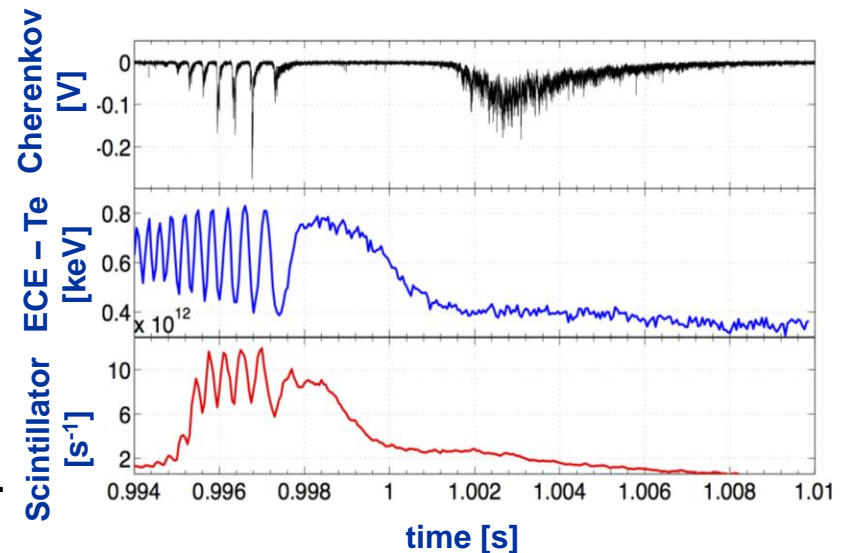
- Cherenkov probe (EX/P2-49)
- Gamma camera
- Laser Induced Breakdown Spectroscopy

# Cherenkov probe



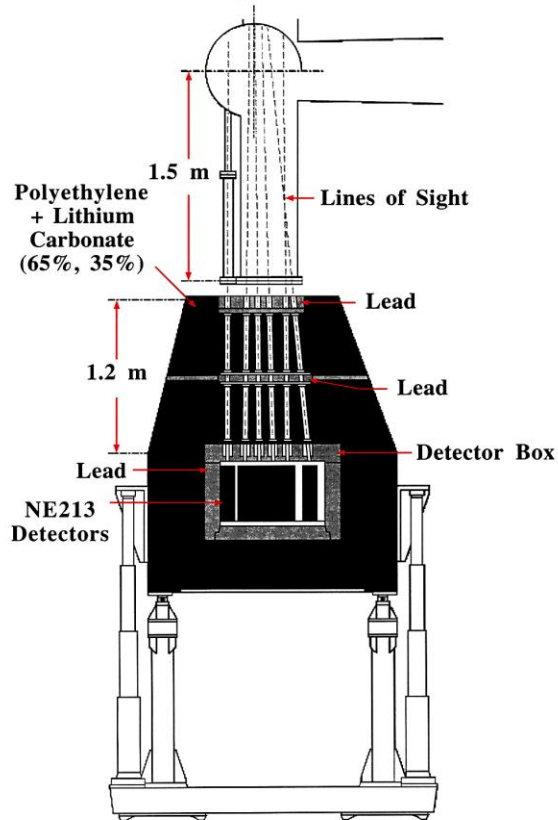
- ☐ Collaboration with NCBJ.
- ☐ Escaping fast electrons detected by Cherenkov radiation emitted in diamond probe.

- ☐ Correlation between Cherenkov signal and magnetic island rotation.
- ☐ Modelling and simulations (HMGC).



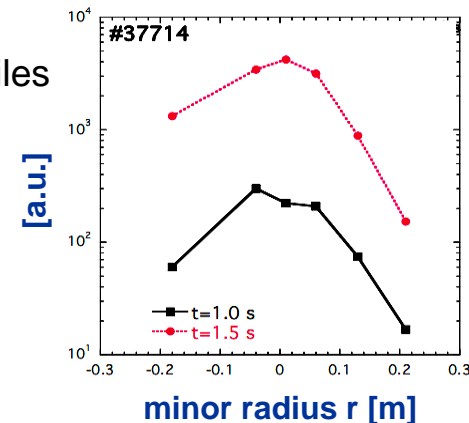
☐ Loss of confinement of fast electrons in the presence of high amplitude magnetic islands.

**Causa F. IAEA EX/P2-49 (2014)**



- ☐ Gamma-ray camera for in-flight runaway electrons emission produced by in-plasma bremsstrahlung.
- ☐ Six radial lines of sight equipped with liquid organic scintillators (NE213).
- ☐ n/ $\gamma$  discrimination in conditions of very high count rate.

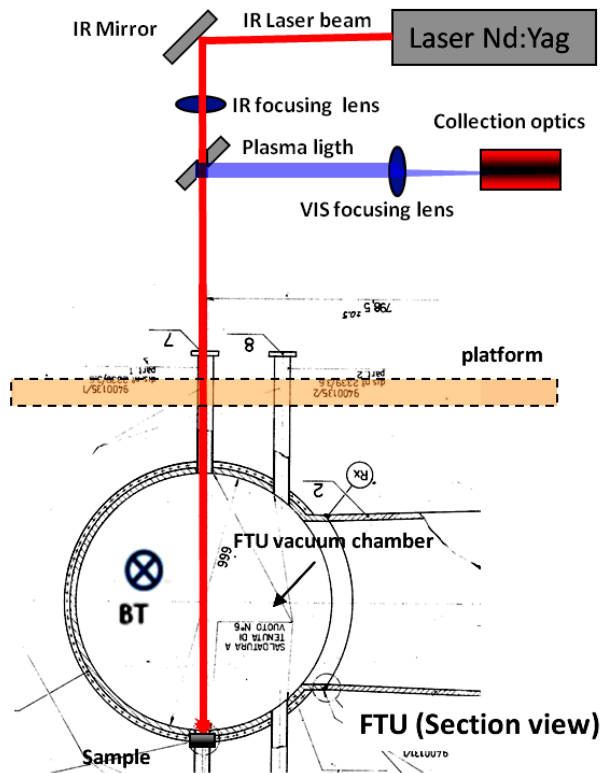
Hard x-ray profiles



☐ Study of the RE population during the current ramp-up, flat-top and ramp-down phases with sub-ms time resolution.

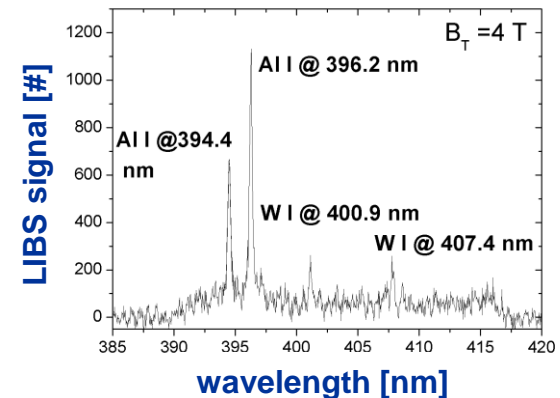
Marocco D., SOFT P2.046 (2014)

# Laser Induced Breakdown Spectroscopy



- ❑ Laser Induced Breakdown Spectroscopy measurements performed on samples placed in FTU vacuum with toroidal field on (up to 4 T).
- ❑ Experiments demonstrate the feasibility of in situ LIBS diagnostic of surface composition.

Sample W-Al-C



❑ Useful information on the surface elemental composition and fuel retention in present and future tokamaks, such as ITER.

Maddaluno G., EPS P5.102 (2013)

- ❑ **Pucella G.**, “Overview of the FTU results”, **OV/5-4**
- ❑ **Mazzitelli G.**, “Thermal loads on FTU actively cooled liquid lithium limiter”, **EX/P2-46**
- ❑ **Sozzi C.**, “Experiments on magneto-hydrodynamics instabilities with ECH/ECCD in FTU using a minimal real-time control system”, **EX/P2-47**
- ❑ **Carnevale D.**, “Runaway electron control in FTU”, **EX/P2-48**
- ❑ **Causa F.**, “Cherenkov emission provides detailed picture of non-thermal electron dynamics in the presence of magnetic islands”, **EX/P2-49**
- ❑ **Esposito B.**, “On the measurements of the threshold electric field for runaway electron generation in FTU”, **EX/P2-50**
- ❑ **Granucci G.**, “Experiments and modelling on FTU tokamak for EC assisted plasma start-up studies in ITER-like configuration”, **EX/P2-51**
- ❑ **Mazzotta C.**, “Peaked density profiles due to neon injection on FTU”, **EX/P2-52**
- ❑ **Botrugno A.**, “Driving  $m/n=2/1$  tearing instability by neon injection in FTU plasma”, **EX/P2-53**
- ❑ **Nowak S.**, “(N)TM onset by central EC power deposition in FTU and TCV tokamaks”, **EX/P2-54**